Extended Parallel Imaging in Alternating-SSFP fMRI

Tiffany Jou[1], Joseph Y Cheng[2], Chris Bowen[3], Michael Lustig[4], and John M Pauly[1]
[1]*Electrical Engineering, Stanford University, Stanford, CA, United States,* [2]*Radiology, Stanford University, Stanford, CA, United States,* [3]*Radiology, Dalhousie University, Halifax, NS, Canada,* [4]*Electrical Engineering and Computer Sciences, UC Berkeley, Berkeley, CA, United States*

Introduction By using RF catalyzation to alternate between two RF phase-cycling steady states (180° and 0°), fat-suppressed Alternating-SSFP (alt-SSFP) recovers banding artifacts in conventional Passband Balanced-SSFP (pb-SSFP) and allows for whole-brain fMRI in a single functional run[1,2]. Alt-SSFP is a promising alternative to conventional GRE-EPI due to its small-vessel BOLD sensitivity, reduced image distortion, and reduced signal dropout as a result of short T_R and rapid excitation. Higher acceleration is desired to increase imaging coverage, spatial resolution (to resolve the high small vessel sensitivity), temporal resolution, or for allowing more phase-cycling angles to be acquired for increased uniformity in spatial sensitivity. In this work, we demonstrate that due to the offset banding patterns of different phase-cycling, the coil sensitivity maps of alternate phase-cycling volumes can be used as additional maps[3,4] to enhance the conditioning of the parallel imaging reconstruction of the alt-SSFP phase-cycled images.

Methods Measurements were made on a GE Discovery MR750 3T scanner using a 32-channel head coil. A 3D multi-shot fly-back EPI sequence with an echo train length of 4 was used with the following parameters: T_R = 14.3 ms, FOV = 240 x 240 x 66 mm^3, 3 mm isotropic resolution, flip angle = 35°, receiver bandwidth = ±62.5 kHz. A true-null spatial-spectral pulse was used for fat-suppression[2]. In order to assess high acceleration factors, undersampling was limited to only the ky direction. Each 3D volume was 4x uniformly undersampled in the phase-encode direction to achieve an equivalent volume time of 3.46 s. Data was retrospectively discarded for the 8x acceleration case.

Fully sampled reference scans of both phase-cycles are acquired at the beginning of the functional run for GRAPPA[5] reconstruction. Instead of reconstructing the two phase-cycling volumes using GRAPPA kernels derived separately from the two reference volumes, we propose that the GRAPPA kernel for each phase-cycling volume can be extended by concatenating the two phase-cycling k-space volumes in the coil dimension (Fig 1). This results in double the number of coil channels and double the number of interpolation weights for each phase-cycling volume, providing additional shared information to boost image SNR and temporal SNR of the fMRI time course. In alt-SSFP fMRI, it is essential to avoid the mixing of contrast between transition band and passband regions when combining the reconstructed different phase-cycling volumes. Therefore, Maximum Intensity Projection (MIP) is then used to combine the two 3D volumes into one temporal volume in the fMRI time course.

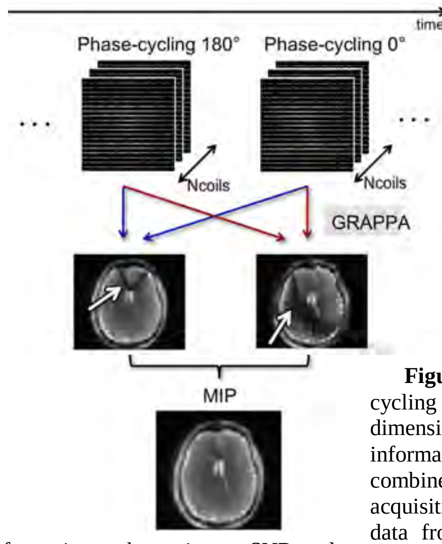

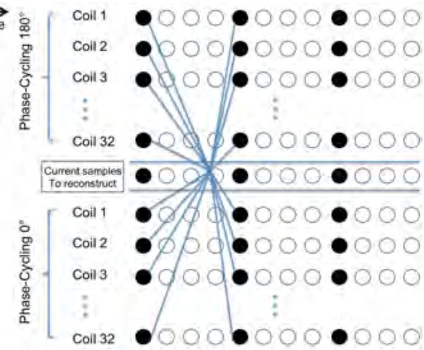

Figure 1 (left) The k-space of the two phase-cycling volumes are concatenated in the coil dimension prior to GRAPPA reconstruction to allow information to be shared. MIP is then used to combine every two alternating phase-cycling 3D acquisitions. **(top)** For each phase-cycling volume, data from 32 coils of both phase-cycling 0° and phase-cycling 180° are used for interpolation using GRAPPA weights computed from fully sampled reference scans.

The GRAPPA weights were used to derive coil sensitivity maps[6] for visualization in Figure 2. G-factor maps were derived using the Pseudo Multiple Replica method[7] to estimate the degree of noise amplification associated with the reconstruction method and acceleration factor.

Visual stimulus experiments were performed. Subjects were scanned while receiving alternating left versus right visual field stimulation. Trial timing was cued by visual stimulus using PsychoPy and PsychToolbox. FSL was used for fMRI data analysis. Temporal SNR maps were generated by dividing mean signal level by standard deviation of the GLM residuals.

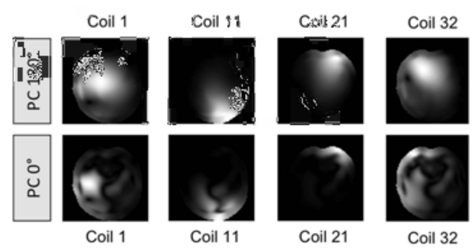

Figure 2 Select coil sensitivity maps estimated using GRAPPA weights[6] after concatenation in the coil dimension of the two 32-channel phase-cycling k-space volumes.

Results and Discussion Incorporating alternate phase-cycling banding maps as additional sensitivity maps results in much lower g-factor values at high acceleration factors (Fig 3). Temporal SNR maps from a visual stimulus fMRI scan show increased signal stability for the combined 64 coils case, which is essential for reliable functional analysis (Fig 4). SENSE can not be used since the algorithm results in a mixing of transition band and passband signal which is undesirable for alt-SSFP fMRI. Therefore, since MIP is the current preferred method of image combination, this coil concatenation method is compatible with parallel imaging methods that process coils separately and enable final MIP of the two phase-cycling volumes.

Conclusion This work shows that the offset banding patterns in different phase-cycling volumes of alt-SSFP can be used to extend the GRAPPA kernel for the reconstruction of each phase-cycling volume. This increases temporal SNR for alt-SSFP fMRI in highly accelerated cases. Future work will be done to optimize the sampling to better take advantage of this coil combination method.

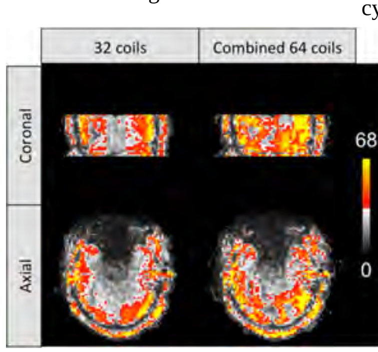

Figure 4 tSNR maps of representative axial and coronal slices from visual stimulus fMRI scan with 8x acceleration show increased tSNR for the combined 64 coils case. Axial tSNR maps correspond nicely to estimated g-factor maps of the same slice (Fig 3).

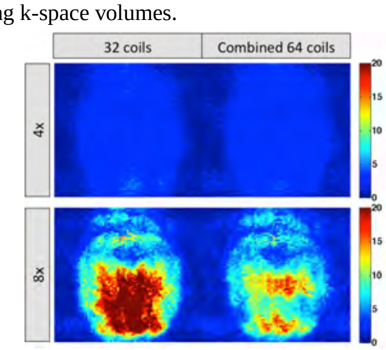

Figure 3 g-factor maps for different acceleration factors. For 4x acceleration, both cases perform similarly. For a higher acceleration of 8x, the combined 64 coils case has much lower g-factor values overall.

References [1] Patterson, et al. 20th ISMRM (2012), p2309; [2] Jou, et al. 22nd ISMRM (2014), p261; [3] Lustig, et al. 13th ISMRM (2005), p504; [4] Lustig, et al. US Patent 7,132,828 (2005); [5] Griswold, et al. MRM (2002), 47:1202-1210; [6] Uecker, et al. MRM (2014), 71:990-1001; [7] Robson, et al. MRM (2008), 60:895-907